The role of linker DNA in chromatin fibers

Brouwer, T.B.

Chapter 6

Mechanical and Structural Properties of Archaeal Hypernucleosomes

Many archaeal species express homologs of eukaryotic histones H3, H4, H2A and H2B, which organize the genome and play a key role in gene regulation. The structure and function of archaeal histone-DNA complexes remain however largely unclear. Recent X-ray crystallography studies of *Methanothermus fervidus* histone HMfB bound to DNA fragments show formation of hypernucleosomes consisting of DNA wrapped around an 'endless' histone-protein core. Such a structure is in line with analysis of digested nucleoprotein complexes suggesting that these complexes consist of an integer number of dimeric units of archaeal histones *in vivo*. However, if and how such a hypernucleosome structure assembles on a long DNA substrate and which interactions provide for its stability, remains unclear.

Here, we describe micromanipulation studies of complexes of the *M. fervidus* histones HMfA and HMfB with single DNA tethers. Our experiments show hypernucleosome assembly which results from cooperative binding of histones to DNA, facilitated by stacking interactions between neighboring histone dimers. Furthermore, rotational force spectroscopy demonstrates that the HMfB-DNA complex has a left-handed chirality, but that torque can drive it in a right-handed conformation. The structure of the hypernucleosome thus depends on stacking interactions, torque, and force. *In vivo*, such modulation of the archaeal hypernucleosome structure may play an important role in transcription regulation as a responsive to environmental changes.

Significance statement

Archaea are highly relevant as they are one of the main pillars of life and form a link between the last universal common ancestor in life on earth (LUCA) and Eukaryotes becomes more unequivocal. In eukaryotes, histones play an important role in genome compaction and gene regulation. Archaea also express histones, but they lack a key feature of the eukaryotic histone: the N-terminal tail, important in eukaryotic transcription regulation. With no N-terminal tail, Archaea must have an alternative way of modulating DNA accessibility, although the archaeal transcription regulation mechanisms are poorly understood. We investigated how archaeal histones compact DNA. Its mechanisms of compaction are suggestive of primordial bacterial-like transcription regulatory mechanisms preceding eukaryotic regulatory mechanisms.

This chapter is based on: Henneman B., Brouwer T. B., van Emmerik C., van der Valk R. A., Timmer M., Kirolos N., van Ingen H., van Noort S. J. T., Dame R. T.: Mechanical and Structural Properties of Archaeal Hypernucleosomes, *submitted*.

6.1 Introduction

Dynamic genome organization is a prerequisite for a compact yet active genome throughout all domains of life. Current views on evolution agree that eukaryotes are part of the branch of Archaea, which are single-cellular organisms that share many cellular mechanisms with Eukaryotes [1–4]. Eukaryotes use histones, which wrap DNA into nucleosomes to compact and functionally organize their genomes. These histones have N-terminal tails that can be post-translationally modified, which changes their physico-chemical properties, and is key in defining the functional chromatin state [5]. Most archaeal species express rudimentary homologs of eukaryotic histones with the characteristic histone fold [6–8], but lack the N-terminal tail [9–13]. In addition to histones, Archaea express other small architectural proteins, nucleoid-associated proteins (NAPs). These NAPs are also involved in genome organization and may complement or compete with histones to regulate genes [14, 15].

The prototypical archaeal histones are HMfA and HMfB from *Methanothermus fervidus* [16]. HMfA and HMfB are homologs of eukaryotic histones in terms of sequence and structure [13]. HMfA and HMfB share 84% sequence identity. These proteins are expressed at varying ratios as a function of growth phase [17]. Although estimates of absolute expression levels of individual histones are lacking, HMfA is prevalent during exponential growth (1.5× the amount of HMfB), and present in equal amounts as HMfB during stationary growth [17]. This might imply that these proteins have evolved different DNA binding properties – and correspondingly distinct functions – in the cell. HMfA and HMfB are capable of forming homo- and heterodimers, which subsequently can form larger structures [17–20]. The binding of HMf dimers to DNA results in bends in DNA at low protein concentrations, and has been reported to yield beads-on-a-string nucleosome-like structures at higher protein to DNA ratios [16]. HMf proteins bind preferentially to intrinsically curved DNA sequences *in vitro* [21]. There is currently no evidence of the existence of specific DNA sequence signatures that enhance histone binding *in vivo*, although studies in *Methanothermobacter thermautotrophicus* and *Thermococcus kodakarensis* indicate that repetitive motifs of AT and GC base pair steps favor histone positioning [22]. These motifs facilitate the distortion needed for DNA wrapping. Systematic evolution of ligands by exponential enrichment (SELEX) experiments have yielded two high-affinity DNA binding sequences for HMfB *in vitro* [23]. Binding of HMf proteins to this sequence yields nucleosome-like structures, in which 60 base pairs of DNA is proposed to be wrapped around a tetrameric protein core composed of two interacting HMf dimers [24]. Here, we will refer to the DNA compaction mode of HMf proteins as wrapping, even when the DNA is wrapped less than one turn.

The histone tetramer model is supported by micrococcal nuclease (MNase) digestion studies of chromatin from *Haloferax volcanii*, which yield undigested

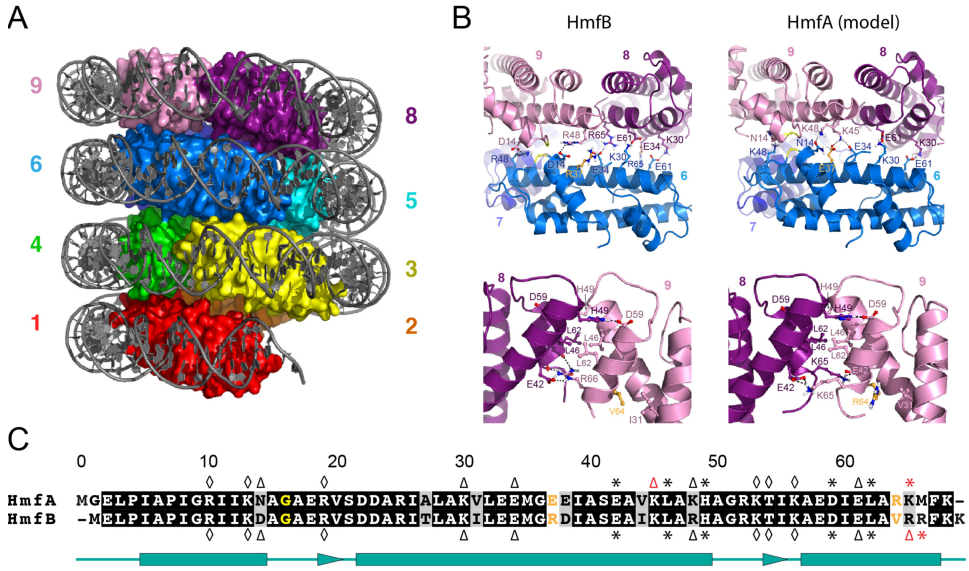

Figure 6.1
The hypernucleosome and *Methanothermus fervidus* histones HMfB and HMfA. a) The HMfB hypernucleosome structure as described by Mattiroli *et al.* (PDB: 5T5K [25]). Figure taken from Henneman *et al.* 2018 with permission [26]. B) Hypernucleosome interfaces of HMfB (left; water-refined and starting from the 5T5K structure) and HMfA (right; water-refined and starting from the homology model). Top panels show the stacking interface, bottom panels show the tetramer interface. Interacting residues are labeled; hydrogen bonds are shown by dashed lines. Important residue differences between HMfA and HMfB are colored in orange. The closely packed residues G16 in the stacking interface are shown in yellow spheres (Cα only). C) Sequence alignment of HMfA and HMfB. Conserved residues are shown in black boxes, conservative changes in grey and non-conservative changes in white boxes. Residues are numbered according to HMfB sequence. The two sequences are 84% identical and have 94% similarity. Residues directly contacting the DNA are indicated with diamonds (◊), residues forming the tetramerization interface are marked with asterisks (∗) and stacking residues are indicated with triangles (△) for HMfA (top) and HMfB (bottom). Differences in interacting residues between HMfA and HMfB are indicated with red symbols. Important residue differences between HMfA and HMfB are colored in orange and G16 residues are shown in yellow, matching panel B.

DNA fragments 60 base pairs in size [22, 27]. However, the histone tetramer model has been challenged by the results of similar studies in *T. kodakarensis*, which yield DNA fragments ranging from 30 – 450 base pairs in 30 base pairs increments [28]. The sizes of these DNA fragments were interpreted as reflecting the existence of histone multimers of varying sizes bound along the genome. A notable recent crystallography study of HMfB on 90 base pair DNA fragments supports the formation of a multimeric histone filament established by interactions between adjacent histone dimers and of wrapping of DNA fragments around an endless protein core, creating a quasi-continuous superhelix (Figure 6.1A) [25]. This structure is referred to as the hypernucleosome [26]. The hypernucleosome is left-handed like the eukaryotic nucleosome, although it has been reported that archaeal histones can accommodate both left- and right-handed wrapping configurations [20, 29, 30]. It was proposed that hypernucleosomes are not just held together by interactions between adjacent dimers, but also by stacking interactions between the layers of dimers within the hypernucleosome (Figures 6.1B and 6.1C) [26]. The disparate findings from *H. volcanii* and *T. kodakarensis*, as well as the crystal structure of HMfB-DNA complexes, indicate that molecular insights into the role of histones in archaeal chromatin organization are important for understanding archaeal genome compaction.

In this study, we provide direct evidence of hypernucleosome formation and its capability of transitioning in handedness. HMfA and HMfB homodimers exhibit subtle differences in amino acid composition, resulting in different stacking energies in the hypernucleosomes. This results in different stabilities of the hypernucleosome, which may be the key mechanism of transcription regulation in Archaea.

6.2 Results

6.2.1 Both HMfA and HMfB cooperatively compact DNA

To determine the degree of DNA compaction by HMfA and HMfB, we performed Tethered Particle Motion experiments (TPM) [34]. Here, the Root Mean Squared displacement (RMS) of a bead connected to a surface-attached DNA tether provides a quantitative readout of DNA conformation (Supplementary Figure 6.S1A). We investigated the binding of HMfA and HMfB to a 685 base pairs DNA molecule containing a random, naturally occurring sequence (*see* Materials and Methods). We observed an abrupt and drastic reduction in RMS of the DNA tether over a narrow concentration range during titration of both proteins, which indicates that DNA compaction by both HMfA and HMfB is highly cooperative. Such cooperativity is due to either direct protein-protein interactions or facilitated protein-DNA binding through structural effects of adjacently bound HMfA or HMfB proteins [20, 35] (Figure 6.2).

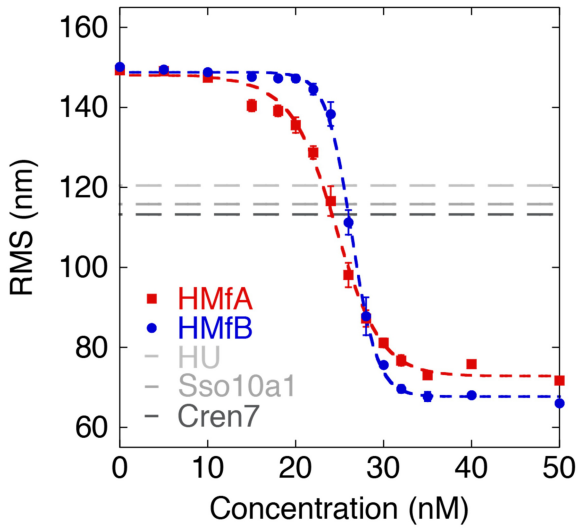

Figure 6.2
***Methanothermus fervidus* histone proteins HMfA and HMfB cooperatively compact DNA in Tethered Particle Motion experiments.** Root mean square displacement (RMS) excursion of the bead for HMfA and HMfB on a DNA substrate is shown as a function of protein concentration. Dashed lines are to guide the eye. Error bars indicating the standard error of the data points ($N \geq 100$) are small and mostly hidden behind the data points. In grey, saturation levels of the bacterial NAP HU and archaeal NAPs Sso10a1 and Cren7 – which are known to organize and compact DNA – are indicated, as reported by Driessen *et al.* 2014, Driessen *et al.* 2016 and Driessen *et al.* 2013 [31–33].

As a dimer, HMf proteins bend DNA to an angle that is similar to those induced by other DNA-bending proteins, such as the bacterial NAP HU and the archaeal NAPs Cren7 and Sso10a1 [16, 31–33, 36, 37]. These proteins reduce the RMS of a 685 base pairs DNA substrate from 150 to 110-120 nm at saturating protein concentrations [31, 32]. A much stronger reduction in RMS down to 70 nm was observed for HMfB and $\sim$ 75 nm for HMfA. The extent of this change cannot be explained by DNA bending induced by individual HMf dimers. The high degree of DNA compaction together with the pronounced binding cooperativity suggests adjacent packing of HMfB (and HMfA) proteins that together wrap DNA into multiple turns. By determining the maximum deflection of the bead in TPM, we found an end-to-end distance of 24 ± 4.7 nm for the HMfB-DNA complex at saturating protein concentrations for this specific DNA substrate (Supplementary Figure 6.S1). This number agrees with the theoretical end-to-end distance of the hypernucleosomal structure observed in the crystallography studies [25]. Both HMf proteins bind to DNA in a cooperative manner, but HMfB shows a more pronounced cooperativity than HMfA. Differences in the stacking interface or tetramerization interface of

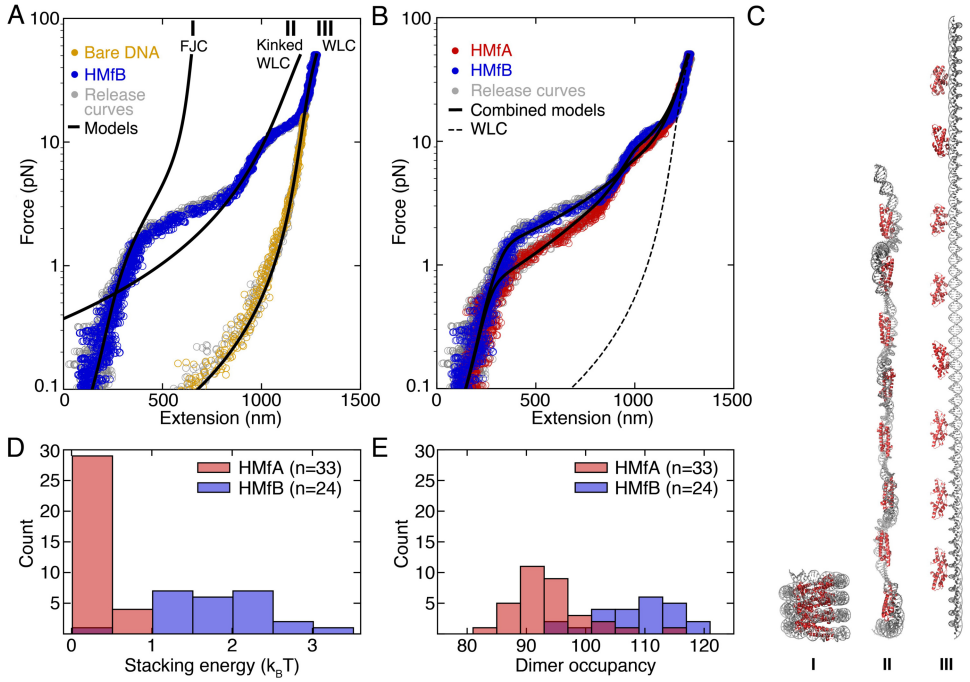

Figure 6.3
Force spectroscopy experiments on the hypernucleosome reveal stronger stacking in HMfB tethers than in HMfA tethers. A) Force spectroscopy on a HMfB-DNA complex (blue dots) at 100 nM of HMfB reveals three levels of compaction. A bare DNA molecule is shown in yellow dots. We fitted different parts of the curve to a freely-jointed chain (FJC) (I), kinked worm-like chain (WLC) (II), and WLC (III). The release curves overlapped with the stretch curves, which indicates that HMfB-DNA the stretch-release cycle was in equilibrium. B) Comparison between HMfA hypernucleosomes (red dots) and HMfB hypernucleosomes (blue dots). The WLC model for bare DNA was added as a reference (dashed black line). The free energy for dimer stacking and DNA wrapping was extracted by fitting the unfolding model (black lines). C) Structural models of three states of the HMfB-DNA complex corresponding to the model fit in A, illustrating a 7-fold compaction of the hypernucleosome compared to bare DNA. D) Histogram of stacking energies of HMfA and HMfB. E) Histogram of HMfA and HMfB dimers occupancy.

HMfA and HMfB may underlie the difference in DNA compaction (Figures 6.1B and 6.1C).

6.2.2 HMfB organizes long DNA tethers into endless hypernucleosomes

The mechanical stability of the hypernucleosome was further investigated by force spectroscopy. HMfB hypernucleosomes were reconstituted *in vitro* on a torsionally unconstrained DNA construct, at 100 nM HMfB, well above the K_d. Hence, we expect full coverage of the DNA. Force spectroscopy

revealed characteristic reversible force-extension curves (Figure 6.3A, 6.3B). Binding of HMfB resulted in a large compaction of the DNA. The absence of hysteresis indicates that the manipulation of the HMfB-DNA complex occurs in thermodynamic equilibrium: stretch-release cycles could be repeated multiple times without qualitative changes in the data. The force-extension curve of the HMfB-DNA complex showed three regimes of extension (Figure 6.3A). In regime I, at forces below 1 pN, the force-extension curve featured a small extension and a high stiffness. In regime II, between 2 and 10 pN, the tether is longer and appears to be less stiff than in regime I. In regime III, at forces above 20 pN, the extension of the complex follows that of bare DNA, which is stiffer than the complex in regime II. Most of the force-extension curve of the HMfB-coated DNA could be captured in these three regimes, and we interpret the intermediate parts as transitions between these regimes.

We modeled the two most extended structures, in force regime II and III, with kinked and regular worm-like chains (WLCs). In regime III the complex followed the force-extension curve of bare DNA with a persistence length of 50 nm. For regime II, we fitted the same contour length and a persistence length of approximately 4 nm, suggesting a much more flexible tether. The most compacted structure, regime I, could not be modeled by a WLC and shows a linear extension between 0.1 and 2 pN. We used the linear part of a freely-jointed chain (FJC) to describe this regime of the force-extension curve.

The mechanical properties of the complex suggest three different structures of the tether. Stacking of HMfB dimers into a hypernucleosome would create a relatively stiff structure that can only be stretched to a limited extent without breaking the protein-protein stacking interactions. Based on the crystal structure of the HMfB hypernucleosome [25], we expect an approximate height of 4 nm per dimer for the most condensed structure (Figure 6.3C, I). When the stacking interactions are broken due to excessive force, individual dimers may remain bound to the DNA. Such a structure would have a much larger extension per HMfB dimer than the stacked hypernucleosome. If all DNA-protein contacts remain intact, the DNA follows a highly curved trajectory (Figure 6.3C, II). Such curved DNA results in a decrease of the apparent persistence length [38, 39], which is consistent with the observed force-extension relation in regime II. Increasing the force further breaks protein-DNA interactions to yield an unperturbed DNA trajectory (Figure 6.3C, III), which would have similar mechanical properties as bare DNA. Indeed, at forces larger than 20 pN the force-extension curve overlaps with that of DNA. Thus, the experimental force-extension curves suggest a two-step transition from a hypernucleosome into a fully stretched DNA tether.

For a more quantitative analysis we developed a statistical mechanics model that includes the transitions between the three structures, as described in materials and methods. Release curves fully overlapped with the stretch curves. The absence of hysteresis in all curves indicates that all transitions

are in thermodynamic equilibrium, allowing an equilibrium model to describe the transitions between the states. In analogy with the forced unfolding of eukaryotic chromatin [40], we modeled the entire force-extension curve as a linear combination of the extension of individual dimer-DNA complexes in either of the three states supplemented by a small fraction of bare DNA (*see* Materials and Methods for model details). For every dimer that binds to the DNA tether, the extension changes and the free energy is reduced by a binding and/or stacking energy. For each dimer in state II, we imposed a deflection angle of 10 degrees resulting in a reduction of the persistence length as described by Kulić and Schiessel [38].

The force-induced transitions between all three states of the HMfB-coated DNA tether were adequately captured by the model (Figure 6.3B). The first transition (I to II) at 2 pN indicates a stacking energy of $1.8 \pm 0.7\ k_{\mathrm{B}}T$, which indicates that the stacked hypernucleosome is easily disrupted by force (Figure 6.3D). Such unstacking yielded a lengthening of the tether of ~ 500 nm. Unwrapping of the DNA from the dimers at 10 pN takes more energy, $8.7 \pm 0.9\ k_{\mathrm{B}}T$, and increases the extension of the tether by ~ 200 nm. These transitions appear as gradual changes in extension, likely because of the non-cooperative behavior of the large number of dimers, the small changes in extension per dimer and the fast kinetics. For multiple tethers, we fitted an average of 108 ± 7 dimers per tether. A footprint of 30 base pairs per HMfB dimer would allow 121 dimers to bind this DNA molecule. It therefore appears that the DNA molecule is not fully saturated, implicating defects in stacking of the hypernucleosome (Figure 6.3E). Interestingly, the fitted number of dimers did not change in multiple stretch and release curves of the same hypernucleosome, suggesting that the dimers remain bound to and positioned on the DNA, even at high forces.

TPM experiments showed that HMfB compacts DNA slightly more than HMfA (Figure 6.2). In force spectroscopy, the force-extension curves for HMfA-DNA complexes were similar to those for HMfB-DNA complexes (Figure 6.3B), although the transitions between stacked and unstacked states occurred at lower forces, *i.e.* at 0.5 rather than 2 pN. Correspondingly, we found a smaller stacking energy and dimer occupancy for the HMfA-DNA complex compared to the HMfB-DNA complex, but a similar wrapping energy (Figure 6.3D, 6.3E). The fitted stacking energy, wrapping energy, and dimer occupancy is summarised in Table 6.1. The high similarity in stiffness and extension of the complexes at forces below the unstacking transition (I to II) and the similar wrapping energy after unstacking, highlights the universality of the hypernucleosome structure, whereas the difference in stacking energy and occupancy clearly distinguishes the mechanical properties of the protein-DNA filaments formed by the two homologs. This may be biologically relevant as differences in mechanical stability may modulate the balance between gene compaction and accessibility *in vivo*.

	stacking energy (mean ± SD)	wrapping energy (mean ± SD)	dimer occupancy (mean ± SD)
HMfA	0.3 ± 0.2 k_BT	9.0 ± 2.0 k_BT	94 ± 7 dimers
HMfB	1.8 ± 0.7 k_BT	8.7 ± 0.9 k_BT	108 ± 7 dimers

Table 6.1
Mean stacking energy, wrapping energy and dimer occupancy of HMfA and HMfB.

6.2.3 Stacking interactions mediate hypernucleosome formation

The basis for stacking of HMfA and HMfB homodimers lies in their primary structure. We analyzed both histones in terms of interacting residues in the hypernucleosome structure(Figure 6.1C). Using water refinement with HADDOCK [41] on the HMfB hypernucleosome crystal structure and modeling the HMfA hypernucleosome structure based on that same crystal structure, we were able to identify the possible stacking interactions within the hypernucleosome. For HMfB, we determined interactions between R48-D14, K30-E61 and E34-R65. For HMfA, we found homologous interactions between K31-E62 and E35-K62. Thus HMfB has 1 stacking interaction more than HMfA. The common stacking interactions of both proteins have a similar number and type of hydrogen bonds. When we compare the theoretical total free energy of all interface residues (stacking interfaces and dimer-dimer interfaces including hydrophobic interactions), we surprisingly find that HMfA contacts are energetically more stable than HMfB contacts. Reduced repulsive forces between the HMfA dimers, because of the charge swap at position 37 and the lack of positive charge at position 69, also favor a more stable HMfA complex. However, at HMfB position 64, there is a valine residue that features a hydrophobic interaction with I31, whereas HMfA has an arginine at this position (Figure 6.1C). The large size of this residue disrupts the hydrophobic interaction. This may make the C-terminal α-helix of HMfA more flexible, leading to a less compact and less stable hypernucleosome. Earlier studies support this interpretation, as a V64R mutation in HMfB leads to reduced electrophoretic mobility of the histone-DNA complex and a slightly impaired nucleosome formation [42–44].

6.2.4 The hypernucleosome forms a left-handed structure on DNA

Wrapping DNA into a hypernucleosome imposes a distinct chirality. To reveal handedness and torsional stiffness of the hypernucleosome, we used rotational force spectroscopy on a torsionally constrained HMfB-DNA complexes. As opposed to the experiments described in the previous section, the hypernucleosome was unable to release torsional stress by swiveling around the attachment

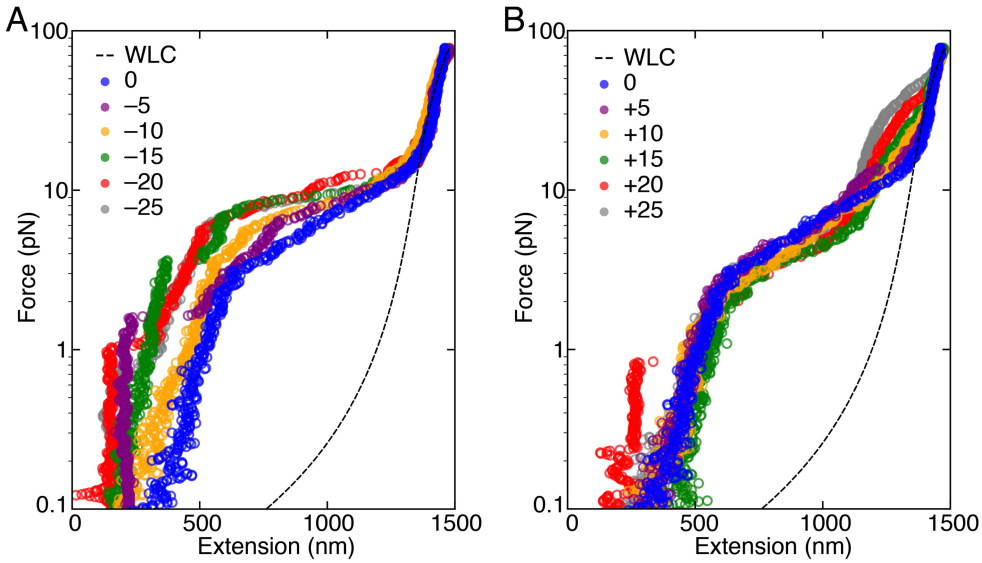

Figure 6.4
Stretching a torsionally constrained HMfB-DNA complex reveals left-handedness of the hypernucleosome, and shows increased affinity of HMfB dimers for positively twisted DNA. A) Negative twist as a result of 5-25 rotations increases the unstacking force of the hypernucleosome. In addition, excess negative twist causes the HMfB-DNA complex to buckle, resulting in a dramatic decrease of its extension. Both observations point to the left-handedness of the hypernucleosome. The unwrapping transition appears largely unaffected, resulting in a continuous decondensation of the tether around 10 pN. B) Positive twist as a result of 5-25 rotations recovers the unstacking plateau. Strikingly, positive twist increases the rupture force of the unwrapping transition of HMfB dimers. An increasing force is necessary to reverse the bending effect of HMfB dimers on DNA. At very low forces the beads appear to stick to the cover slip for certain curves (-5, -20, and +20 rotations, especially).

point in this experiment. The resulting torque could stabilize the HMfB-DNA hypernucleosome when stretched.

We monitored the extension of the hypernucleosome at a constant force, when applying negative (Figure 6.4A) and positive (Figure 6.4B) twist. The force plateau that represents the unstacking transition shifted up to 10 pN for negatively twisted complexes. As more force is required to unstack the hypernucleosome, the energy for the unstacking transition is increased. Large amounts of negative twist compacted the HMfB-DNA complex by buckling the hypernucleosome at forces below 1 pN. The second transition, from wrapped to unbent DNA, appeared unaffected by negative twist. Positive twist, on the other hand, only marginally extended the range of the unstacking transition to 2-10 pN. Such behavior is characteristic of a left-handed structure, and in agreement with the HMfB-DNA co-crystal structure [25]. Strikingly, the bent

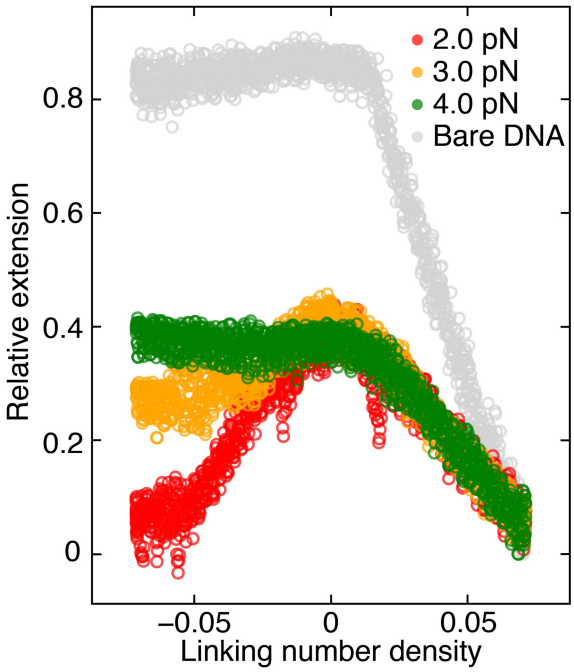

Figure 6.5
Torque stabilizes the hypernucleosome and reveals a right-handed chirality of unstacked HMfB-DNA complexes. A torsionally constrained HMfB hypernucleosome was compacted by twisting the molecule under constant force. At 2.0 pN, both positive and negative twist reduced the extension, presumably by buckling. At higher forces, negative twist caused the HMfB dimers to unwrap from the DNA, which induced stretching of the HMfB-DNA complex. These measurements suggest that the unstacked HMfB-DNA complex is right-handed. As a reference, we included a twist-extension curve of bare DNA at 1.0 pN. Note that the slope for the HMfB-DNA complex is much smaller than that of bare DNA.

DNA was stabilized by positive twist, but not by negative twist. Thus, it appears that unstacked HMfB dimers can better accommodate positive twist than bare DNA. In accordance, the affinity for HMfB dimers increased when overtwisting the DNA.

6.2.5 Unstacked HMfB-DNA complexes impose a right-handed DNA structure

The unstacking transition of a torsionally constrained hypernucleosome features an increased and more gradual force plateau compared to a torsionally unconstrained hypernucleosome (Supplementary Figure 6.S2). As a result, the unstacking transition merges with the transition that we attribute to unwrapping DNA from the HMfB dimers (regime II to III in Figure 6.3A). Since HMfB dimers appeared to remain bound to the DNA, the unwrapping of one dimer

would create additional torsional stress, which impedes unwrapping of the next dimer, resulting in an anti-cooperative transition that manifests itself by an increased force range in which unfolding takes place.

When maintaining a fixed force, and monitoring the extension as a function of twist, we were able to determine the handedness of the unstacked HMfB-DNA complex (Figure 6.5). At $F = 2.0$ pN, both negative and positive twist induced a reduction in extension due to buckling of the hypernucleosome structure. Note that the presence of HMfB-induced bends favored plectonemes over DNA melting, which would occur in bare DNA for negative twist at this force. An asymmetry in twist response in HMfB-decorated tethers occurred at $F = 3.0$ pN. At this force, negative twist helped to unwrap the HMfB dimers, increasing the length of the tether. Similar to bare DNA, positive twist induced supercoils in the tether. This implies that the unstacked HMfB-DNA complex formed a right-handed superhelix and that the HMfB dimer DNA complexes were stabilized by positive torque. The force required to completely unwrap the DNA also depended on the applied twist. In this intermediate force regime, HMfB dimers appeared to have a higher wrapping affinity for positively twisted DNA than for negatively twisted or relaxed DNA. This observation was supported by the release curves (Supplementary Figure 6.S3), which showed that positively twisted complexes more readily restack into hypernucleosomes than relaxed or negatively twisted tethers.

The slope of the curve beyond the buckling transitions, as shown in Figure 6.5, reveals more details of the twisted complex. Bare plectonemic DNA reduces its extension by 40-100 nm per rotation, depending on force, as the size of the loop at the tip of the plectoneme decreases with force [45]. For unstacked HMfB-DNA complexes we measured a reduction of the extension of 16 nm per rotation, much lower than bare DNA, which was independent of force. This is consistent with a fixed HMfB-induced bend at the tip of the plectoneme that defines the tip curvature, and thus the geometry of the plectoneme.

6.3 Discussion

The hypernucleosome structure may be a key feature of archaeal chromosome compaction. Here we characterized the structural and mechanical properties of single DNA tethers containing such hypernucleosomes. We found that hypernucleosomes composed of stacked *M. fervidus* histone homodimers HMfA and HMfB compact DNA much stronger than similar DNA-bending proteins. Both HMfA-DNA and HMfB-DNA complexes featured a two-step unfolding mechanism that could be captured quantitatively in the transitions between a hypernucleosome, an array of wrapped dimers that kink the DNA trajectory, and a stretched DNA molecule to which dimers remain bound. HMfB featured a higher stacking energy than HMfA, resulting in a larger occupancy as well as

a higher stability of the hypernucleosome against force.

The stiffness of hypernucleosomes is larger than that of stacked eukaryotic nucleosomes [40]. This may be explained by the different nature of the stacking interactions. Interactions between eukaryotic nucleosomes are known to be mediated by flexible histone tails. Our data suggest that the archaeal hypernucleosome on the other hand is mediated by stacking interactions between the globular histones that form the hypernucleosome. Stacking energies of HMfA and HMfB dimers ($\sim 2\ k_{\mathrm{B}}T$) are much lower than the 17 $k_{\mathrm{B}}T$ that we reported for eukaryotic nucleosome stacking [46]. The unwrapping of DNA from the HMfA and HMfB dimers on the other hand starts at similar forces as the unwrapping of eukaryotic nucleosomes. However, in hypernucleosomes this happened reversibly, whereas nucleosome unwrapping is generally not in equilibrium.

The equilibrium conditions made it possible to capture the entire force-extension curve in a statistical physics model. This worked better for the unstacking transition than for the unwrapping transition. It should be noted though that modeling of the wrapped dimers as kinks in the DNA trajectory might be somewhat naive, as the high occupancy of the DNA yields a dimer-dimer distances that are much smaller than the typical deflection length for which the Kulić and Schiessel model is valid [38]. Moreover, this model assumes a flat one-dimensional kink, while the super-helical structure of the unfolded hypernucleosome may be more complex. A deflection angle (10°), which matched the curves best, is rather small for the 30 base pair footprint of a HMfA or HMfB dimer. Nevertheless, the resulting force dependent reduction of the end-to-end distance matched quantitatively with the force-extension curve. We resolved a clear transition from a flexible (regime II) to a stiffer WLC (regime III), using the same number of dimers as in the unstacking transition at low force, indicating that this unfolding intermediate can be effectively modeled as an array of wrapped dimers.

In the crystal structure, the hypernucleosome compacts DNA in a left-handed manner, which resembles DNA wrapping by eukaryotic histones. In accordance, we found that negative supercoiling stabilized this most compact regime of the HMfB-DNA complex. However, after breaking the stacking by force, a right-handed HMfB-DNA structure was observed. Such a right-handed HMfB-DNA complex has been described previously as a functional form, responding to environmental cues *in vitro* [17, 30]. Depending on conditions, force and torque, a right-handed HMfB-DNA complex may have a biological function in Archaea.

The archaeal genome is also organized by other NAPs. The components of the organizational machinery however differ per phylum, class and order. Histones are found in almost every branch of the archaeal domain. Currently, evidence in support of hypernucleosome formation has only been reported for *M. fervidus* using X-ray crystallography, and for *T. kodakarensis* showing *in*

vivo effects on transcription and MNase digestion results [25, 28]. It is likely though that histones from other species also assemble into hypernucleosomes [26]. Initiation of the hypernucleosome is probably stochastic, and initial complex formation at multiple sites may lead to frustration when two expanding hypernucleosomes meet. Therefore, long stretches of hypernucleosome will probably be rare in the presence of other factors that regulate chromatin structure [47]. Ultimately, long straight hypernucleosomes might clash with physical boundaries of the cell. Such large and highly ordered structures should be visible with microscopic techniques, but empirical evidence for such large filaments is currently lacking [28].

M. fervidus histones form homo- and heterodimers, and, based on sequence similarities, histones from other species may be able to do so as well. The majority of archaeal chromosomes contain genes coding for two or more different histones. This may provide Archaea with a means to regulate gene expression via changing the length and stability of the hypernucleosome in response to growth phase or environmental cues [17]. For Archaea, transcription regulation may follow a variety of mechanisms [48]. For instance, heterodimers may bind to DNA and interact with other heterodimers via one multimerization site, while other sites remain unbound. Homodimers may form hypernucleosomes, which can be interrupted by other homodimers incapable of certain interactions. Furthermore, sequence specificity in certain histone variants may direct histones to specific genomic targets. The emergence of the N-terminal tail has diverted the eukaryotic histone from the archaeal histone, eventually resulting in alternative abilities to regulate genes than in Archaea [26]. The current methods of biological analysis at the single-molecule level allow for detailed, mechanistic measurements that have the potential to shed light on the evolutionary path of genome compaction and transcription regulation.

6.4 Materials and Methods

6.4.1 DNA substrate preparation

For the TPM DNA substrate, a random sequence of 50% GC content (`CGGC GCAAATTCGTGACCAGTTGCATCAGCTGCGTGAGCTGTTTATCGCAGCATCGTAACAGGATAGT GAAGAAGACT`) was cloned into pBR322, as described previously [32], resulting in plasmid pRD121. We used PCR to generate and amplify a 685 base pairs linear substrate (sequence in supplementary material) containing the cloned sequence, using digoxygenin- and biotin-labeled oligonucleotides [34].

For magnetic tweezers a 3646 base pairs DNA fragment based on plasmid pFW01 (pBPCYC1(wt)/3 derivative [49], sequence in supplementary material) was digested with BsaI and BseYI (New England Biolabs). The fragment was isolated using agarose gel electrophoresis and purified using a Promega Wizard SV Gel & PCR cleanup kit. It was subsequently labeled with digoxigenin and

biotin at either end by a Klenow reaction.

For the torsionally constrained construct, pUC18-based plasmid pTB01, (containing 12 repeats of the Widom 601 sequence separated by 25 base pairs of linker DNA [50], sequence in supplementary material), was digested with BsaI and BseYI. The 4092 base pairs digestion product was isolated using agarose gel electrophoresis and purified using a Promega Wizard SV Gel & PCR cleanup kit. Subsequently, a 650 base pairs handle containing multiple digoxigenin- or biotin-modified bases was ligated on each end. Details of both protocols are provided elsewhere [51]. The 4092 base pairs substrate, based on plasmid pTB01, qualitatively behaved the same as the 3646 base pairs pFW01-based substrate. We did not observe different features of the hypernucleosome on this nucleosome reconstitution template.

6.4.2 Tethered Particle Motion

The tethered particle motion experiments were carried out as described previously [52]. The measurement buffer contained 50 mM Tris-HCl, pH 7 and 75 mM KCl. We used an anisotropic ratio cut-off of 1.3 and a standard deviation cut-off of 8% to select single-tethered beads. The end-to-end distance of the DNA substrate was determined by taking the average of the extremities (2.5% largest values) of the deflection of 25 beads in the xy-plane at 50 nM of HMfB and subtracting the radius of the bead (Supplementary Figure 6.S1). The end-to-end distance was obtained by triangular calculation.

6.4.3 Force spectroscopy and rotational spectroscopy

HMfA and HMfB were diluted to 100 nM in measurement buffer. 1 pM DNA substrate was introduced in the flow cell and incubated with histones, following the TPM protocol, but using paramagnetic M270 beads (Dynabeads; Thermo Fisher Scientific, USA) instead of polystyrene beads. Details of the force spectroscopy experiments and the multiplexed magnetic tweezers setup have been described elsewhere [51]. In each measurement, the force was increased exponentially from 0.01 to 40 pN in 70 seconds, and decreased at the same speed.

6.4.4 Quantitative modeling of stretching the hypernucleosome

To interpret the force-extension behavior of the hypernucleosomes, we developed a statistical mechanics model. HMfA and HMfB dimers bound to the DNA were distributed over three conformations, representing different levels of compaction. In the lowest force regime, HMfA and HMfB homodimers assembled into a hypernucleosome. The extension of the hyper-nucleosome was modeled by a

freely-jointed chain (FJC) [53, 54]:

$$z_{\mathrm{FJC}}(F) = L_{\mathrm{dimer}} \left(\coth\left(\frac{Fb}{k_{\mathrm{B}}T}\right) - \frac{k_{\mathrm{B}}T}{Fb} \right), \tag{6.1}$$

where $z_{\mathrm{FJC}}(F)$ is the extension per dimer, b the Kuhn length that characterizes the tether flexibility, F the force, k_{B} Boltzmann's constant, T the temperature, and L_{dimer} the height of a single dimer (when fully wrapped), which was fixed at 4 nm. The FJC was chosen for both its initial linear increase of extension with force, as observed experimentally, and its asymptote to contour length at high force. For low forces ($Fb \ll k_{\mathrm{B}}T$), the FJC describes a Hookean spring with linear extension, and its stiffness k of the stacked fiber is inversely proportional to the effective Kuhn length [53]:

$$k = \frac{3k_{\mathrm{B}}T}{bL_{\mathrm{dimer}}}. \tag{6.2}$$

Note that only the linear part of the FJC, *i.e.* up to an extension up to 2 nm per dimer, mattered, as the dimers unstacked at larger forces. The second force regime is characterized as a beads-on-a-string structure. In this structure, DNA wraps onto non-interacting HMfA or HMfB homodimers resulting in moderate compaction of the fiber. The beads-on-a-string structure was modeled as an extensible worm-like chain (WLC) [40, 55]:

$$z_{\mathrm{WLC}}(F) = L \left(1 - \frac{1}{2}\sqrt{\frac{k_{\mathrm{B}}T}{FP}} + \frac{F}{S} \right), \tag{6.3}$$

in which $z_{\mathrm{WLC}}(F)$ is the extension of an HMf dimer-DNA complex, L is the contour length of the DNA substrate, S the stretch modulus of DNA and P the persistence length. Since the footprint of an HMfB homodimer is 30 base pairs [56], each transition of a dimer from the hypernucleosome into a beads-on-a-string conformation reduces the contour length of the FJC by L_{dimer} and increases the contour length of the WLC by 30 base pairs. Moreover, each HMf dimer that bends the DNA, which reduces the persistence length of DNA to an apparent persistence length P_{app} [38]:

$$P_{\mathrm{app}} = \frac{P}{\left(1 + PN^2 8 \left[1 - \cos\left(\frac{\alpha}{4}\right)\right]/2\right)^2}, \tag{6.4}$$

in which N is the number of dimers in the beads-on-a-string conformation and α is the DNA deflection angle induced by the dimer. In addition, we added a small free energy contribution per kink g_{kink} that is proportional to the square root of force and did not exceed 0.01 $k_{\mathrm{B}}T$ [57]. The model matched the data best using a deflection angle of 10 degrees, which corresponds roughly to the structure depicted in Figure 6.3C.

At high forces, the HMfA and HMfB homodimers appeared to remain bound, but did not bend the DNA. Each transition therefore reduced the number of kinks in the DNA, resulting in an increase of the apparent persistence length to that of bare DNA, for which we used $P = 50$ nm and $S = 1000$ pN [40, 54, 58].

A large number of fiber states j can be defined, reflecting different distributions of each of the three dimer conformations i, representing the hypernucleosome, the beads-on-a-string, or the straight conformation. The total extension $z_j(F)$ of the tether is a linear combination of the extension of each dimer conformation $z_i(F)$ multiplied by the number of dimers n_i in conformation i:

$$z_j(F) = \sum\nolimits_i n_i z_i(F). \tag{6.5}$$

The free energy per dimer in the hyper-nucleosome is given by:

$$\begin{aligned} g_{\mathrm{FJC}} &= \int z_{\mathrm{FJC}}(F)\mathrm{d}F + g_{\mathrm{stack}} + g_{\mathrm{wrap}} = \\ L_{\mathrm{dimer}}\frac{k_{\mathrm{B}}T}{b}&\left(\ln\left(\sinh\left(\frac{Fb}{k_{\mathrm{B}}T}\right)\right) - \ln\left(\frac{fB}{k_{\mathrm{B}}T}\right)\right) + g_{\mathrm{stack}} + g_{\mathrm{wrap}}, \end{aligned} \tag{6.6}$$

using a protein-protein interaction energy g_{stack} and a protein-DNA interaction energy g_{wrap}.

The free energy per dimer in the wrapped and the straight conformation is given by:

$$g_{\mathrm{WLC}} = \int z_{\mathrm{WLC}}(F)\mathrm{d}F = L\left(F - \sqrt{\frac{Fk_{\mathrm{B}}T}{P}} + \frac{F^2}{2S}\right), \tag{6.7}$$

complemented by g_{wrap} for the wrapped conformation. In addition, the work W done by the bead corresponds to:

$$W = \int F(z_j)\mathrm{d}z. \tag{6.8}$$

The total free energy $G_j(F)$ of a particular tether is the work by the bead minus the sum of the free energy contributions of each dimer with an additional free energy contribution for the number of kinks $N \cdot g_{\mathrm{kink}}$ [57]:

$$G_j(F) = W - \sum\nolimits_i n_i g_i(F) + N \cdot g_{\mathrm{kink}}. \tag{6.9}$$

Finally, the force dependent extension of the HMf-DNA complex was calculated as the Boltzmann-weighted mean extension:

$$\langle z_{\mathrm{tot}}(F)\rangle = \frac{\sum_j z_j(F)\exp\left(-G_j(F)/k_{\mathrm{B}}T\right)}{Z} - z_0 \tag{6.10}$$

with partition function $Z = \sum_j \exp\left(-G_j(F)/k_{\mathrm{B}}T\right)$.

Prior to fitting the entire curve, the z-offset z_0 was determined by fitting the WLC for bare DNA at forces over 30 pN. Subsequently, the number of dimers on the DNA was determined based on the maximum compaction of state I and state II. The stiffness k of the hypernucleosome was fixed at 1.2 pN/nm, yielding a good agreement with the data. Since the hypernucleosome unstacked at a relatively low force, fitting this value was problematic. Equation 6.10 was fitted to the force-extension curve in the force range between 0.5 and 55 pN to extract the number of dimers, the stacking energy g_{stack} and wrapping energy g_{wrap} from each curve.

6.5 Acknowledgments

We thank Kathleen Sandman and John Reeve for providing wild type HMfA and HMfB. We thank Helmut Schiessel for fruitful discussions and guidance during the development of the statistical mechanics model. Research in this article is supported by grants from the Netherlands Organization for Scientific Research [VICI 016.160.613] (RTD), [VICI 680.47.616] (JvN), and [VIDI 723.013.010] (HvI), the FOM Foundation for Fundamental Research on Matter program 'Crowd management: The physics of genome processing in complex environments' (RTD) and the Human Frontiers Science program [RGP0014/2014] (RTD).

6.6 Supplementary Material

6.6.1 Sequence of the TPM substrate

5' TTACTTTCACCAGCGTTTCTGGGTGAGCAAAAACAGGAAGGCAAAATGCCGCAAAAAAGGG
AATAAGGGCGACACGGAAATGTTGAATACTCATACTCTTCCTTTTTCAATATTATTGAAGCATT
TATCAGGGTTATTGTCTCATGAGCGGATACATATTTGAATGTATTTAGAAAAATAAACAAATAG
GGGTTCCGCGCACATTTCCCCGAAAAGTGCCACCTGACGTCTAAGAAACCATTATTATCATGAC
ATTAACCTATAAAAATAGGCGTATCACGAGGCCCTTTCGTCTTCAAGAATTCCGGCGCAAATTC
GTGACCAGTTGCATCAGCTGCGTGAGCTGTTTATCGCAGCATCGTAACAGGATAGTGAAGAAGA
CTAAGCTTTAATGCGGTAGTTTATCACAGTTAAATTGCTAACGCAGTCAGGCACCGTGTATGAA
ATCTAACAATGCGCTCATCGTCATCCTCGGCACCGTCACCCTGGATGCTGTAGGCATAGGCTTG
GTTATGCCGGTACTGCCGGGCCTCTTGCGGGATATCGTCCATTCCGACAGCATCGCCAGTCACT
ATGGCGTGCTGCTAGCGCTATATGCGTTGATGCAATTTCTATGCGCACCCGTTCTCGGAGCACT
GTCCGACCGCTTTGGCCGCCGCCCAGTCCTGCTCGCTTCGCTACTTGG 3'

6.6.2 Sequence of the torsionally free substrate

5' ACCGCGAGACCCACGCTCACCGGCTCCAGATTTATCAGCAATAAACCAGCCAGCCGGAAGG
GCCGAGCGCAGAAGTGGTCCTGCAACTTTATCCGCCTCCATCCAGTCTATTAATTGTTGCCGGG
AAGCTAGAGTAAGTAGTTCGCCAGTTAATAGTTTGCGCAACGTTGTTGCCATTGCTACAGGCAT
CGTGGTGTCACGCTCGTCGTTTGGTATGGCTTCATTCAGCTCCGGTTCCCAACGATCAAGGCGA
GTTACATGATCCCCCATGTTGTGCAAAAAAGCGGTTAGCTCCTTCGGTCCTCCGATCGTTGTCA
GAAGTAAGTTGGCCGCAGTGTTATCACTCATGGTTATGGCAGCACTGCATAATTCTCTTACTGT
CATGCCATCCGTAAGATGCTTTTCTGTGACTGGTGAGTACTCAACCAAGTCATTCTGAGAATAG
TGTATGCGGCGACCGAGTTGCTCTTGCCCGGCGTCAATACGGGATAATACCGCGCCACATAGCA
GAACTTTAAAAGTGCTCATCATTGGAAAACGTTCTTCGGGGCGAAAACTCTCAAGGATCTTACC
GCTGTTGAGATCCAGTTCGATGTAACCCACTCGTGCACCCAACTGATCTTCAGCATCTTTTACT
TTCACCAGCGTTTCTGGGTGAGCAAAAACAGGAAGGCAAAATGCCGCAAAAAAGGGAATAAGGG
CGACACGGAAATGTTGAATACTCATACTCTTCCTTTTTCAATATTATTGAAGCATTTATCAGGG
TTATTGTCTCATGAGCGGATACATATTTGAATGTATTTAGAAAAATAAACAAATAGGGGTTCCG
CGCACATTTCCCCGAAAAGTGCCACCTGACGTCTAAGAAACCATTATTATCATGACATTAACCT
ATAAAAATAGGCGTATCACGAGGCCCTTTCGTCTCGCGCGTTTCGGTGATGACGGTGAAAACCT
CTGACACATGCAGCTCCCGGAGACGGTCACAGCTTGTCTGTAAGCGGATGCCGGGAGCAGACAA
GCCCGTCAGGGCGCGTCAGCGGGTGTTGGCGGGTGTCGGGGCTGGCTTAACTATGCGGCATCAG
AGCAGATTGTACTGAGAGTGCACCATATGCGGTGTGAAATACCGCACAGATGCGTAAGGAGAAA
ATACCGCATCAGGCGCCATTCGCCATTCAGGCTGCGCAACTGTTGGGAAGGGCGATCGGTGCGG
GCCTCTTCGCTATTACGCCAGCTGGCGAAAGGGGGATGTGCTGCAAGGCGATTAAGTTGGGTAA
CGCCAGGGTTTTCCCAGTCACGACGTTGTAAAACGACGGCCAGTGCCAAGCTTGCATGCCTGCA
GGTCGACGAGGTGATATTTCCAATTTGGGAAATTTCCCAAATCAGTAATGTAGCCTCTACGGGT
GTCTCTGTCAGCCCCGTGGTCGCCAGCACAGAATGTATCGTACCCCTGAAGGTAGTTTTTTACC
GCCGTGGCACACGATAAAGGTGCACCTTGTGATAATAAGGTGGAAAAATATATATGAAAAAGTG
AAATTGATTGTGGCTGCACTAGGACATCATTATTTCTTACTTGGCTATTTACACGTACTTACGC
TGGCTGTATATCATTTAAGGGGCGGAGGACGAAGAGGACGGACCCGAGATCATCCGGTCCAAGA

AACGGGTCATCCGGTCCTTAGCATTGTCTAGACTATCTAGGGCAGGACGGACATCCACGTGGAA
AGTAGGCATTCCGTTTTCGTCGTCGGGCCCTCCGTAGAAATCCAAGACGTATCTAACTTCCTTG
AAGGTTGGAGGTTGTTGTTCCGCTTTGCGCTCGCCTCGGAGTACAATCCAGTCGTGCCTGTCGA
ATGGTAGTTCTTGGCTAAAATGGGACGGAAACAGTAGGCCGCACAGGTGCATCCAGCGAGCACG
AGGGCTCAATACGCCCGGTTTCCCCATGAATTTCAGCAACTTAGGCTGCACGTGGCTTTCATCT
GTGTGCGGTTTTTCCCATTCGAGCACTTCCTGCCAGCACCCTTCATTTAGAAAGTTGTGGACCT
GCACCATCGACTCCACTGCATCTTCGGCGACTTCGCCGCTACCGCCAATCTTGCCCTTTCTAAC
CATAGCATTGTACATCTGTTGTGGAGAAGGATACTCCCAGAACTCGTTACTGTCTGGACTCTTG
GGGATGCTGGAGATGGTCCGATCAACGGGCAAGTCCATCTTTTGGCCAGGCTGTTTGGATGCTG
CCAACTCCGGCATATTGTTCAGCGGGTTTATTCTATCGTTATCTCCCTGCATAACGGGGCACTC
AGAGGATGGTGGCGACGACGACGACGACTCGTGCATGACTGGGCACCCTGACATGGATGATACT
GCTGCCCCACCAATATCTTTGCCCGTAGTTTTTTGATCTGCCCAAAACCAACCCATTTTTTGTG
AATTCATAGTATCGATACCCTCCTAAGTTTTGTAATCTATAAAGTTAGCAATTTAACTAAGTGT
AAAAACTTAGCTAGCTTACTAAAAAGATAATTACTGAAAAGCTAGCTTGGCCGGATCCGATCGA
CAAAGGAAAAGGGGCCTGTTTACTCACAAGCTTTTTTCAAGTAGGTAATTAAGTCGTTTCTGTC
TTTTTCCTTCTTCAACCCACCAAACGCGTACTTGGTACCAGGAATATATTTCTTTGGGTTAGTC
AAGTACTCTGACATGTTATTTTCGTCCCACAACACGTTTTTCTTGATATTGGCATCTGTGTACG
AATACCCTTCAGCTTGACCAGAGTGTCTGCCAAAGATACCATGCAAGTTTGGACCAACCTTATG
TGGGCCACCCTTTTCCACGGTGTGGCATTGTAGACATCTAGTCTTGAAAAGTGTAGCACCTTTC
TTAGCAGAACCGGCCTTGAATTCAGCCATGGATATATCTCCTTCTTAAAGTTAAACAAAATTAT
TTCTAGATTAGTTAGTTATGGATCCCCGGGTACCGAGCTCGAATTCGTAATCATGGTCATAGCT
GTTTCCTGTGTGAAATTGTTATCCGCTCACAATTCCACACAACATACGAGCCGGAAGCATAAAG
TGTAAAGCCTGGGGTGCCTAATGAGTGAGCTAACTCACATTAATTGCGTTGCGCTCACTGCCCG
CTTTCCAGTCGGGAAACCTGTCGTGCCAGCTGCATTAATGAATCGGCCAACGCGCGGGGAGAGG
CGGTTTGCGTATTGGGCGCTCTTCCGCTTCCTCGCTCACTGACTCGCTGCGCTCGGTCGTTCGG
CTGCGGCGAGCGGTATCAGCTCACTCAAAGGCGGTAATACGGTTATCCACAGAATCAGGGGATA
ACGCAGGAAAGAACATGTGAGCAAAAGGCCAGCAAAAGGCCAGGAACCGTAAAAAGGCCGCGTT
GCTGGCGTTTTTCCATAGGCTCCGCCCCCCTGACGAGCATCACAAAAATCGACGCTCAAGTCAG
AGGTGGCGAAACCCGACAGGACTATAAAGATACCAGGCGTTTCCCCCTGGAAGCTCCCTCGTGC
GCTCTCCTGTTCCGACCCTGCCGCTTACCGGATACCTGTCCGCCTTTCTCCCTTCGGGAAGCGT
GGCGCTTTCTCATAGCTCACGCTGTAGGTATCTCAGTTCGGTGTAGGTCGTTCGCTCCAAGCTG
G 3'

6.6.3 Sequence of the torsionally constrained substrate

5' TCGCGCGTTTCGGTGATGACGGTGAAAACCTCTGACACATGCAGCTCCCGGAGACGGTCAC
AGCTTGTCTGTAAGCGGATGCCGGGAGCAGACAAGCCCGTCAGGGCGCGTCAGCGGGTGTTGGC
GGGTGTCGGGGCTGGCTTAACTATGCGGCATCAGAGCAGATTGTACTGAGAGTGCACCATATGC
GGTGTGAAATACCGCACAGATGCGTAAGGAGAAAATACCGCATCAGGCGCCATTCGCCATTCAG
GCTGCGCAACTGTTGGGAAGGGCGATCGGTGCGGGCCTCTTCGCTATTACGCCAGCTGGCGAAA
GGGGGATGTGCTGCAAGGCGATTAAGTTGGGTAACGCCAGGGTTTTCCCAGTCACGACGTTGTA
AAACGACGGCCAGTGAATTCGAGCTCGGTACCCGGGGATCCTCTAGAGAATATCCCGCCCTGGA
GAATCCCGGTGCCGAGGCCGCTCAATTGGTCGTAGACAGCTCTAGCACCGCTTAAACGCACGTA

CGCGCTGTCCCCCGCGTTTTAACCGCCAAGGGGATTACTCCCTAGTCTCCAGGCACGTGTCAGA
TATATACATCCTGTGCATGTAACTAGAGAATATCCCGCCCTGGAGAATCCCGGTGCCGAGGCCG
CTCAATTGGTCGTAGACAGCTCTAGCACCGCTTAAACGCACGTACGCGCTGTCCCCCGCGTTTT
AACCGCCAAGGGGATTACTCCCTAGTCTCCAGGCACGTGTCAGATATATACATCCTGTGCATGT
AACTAGAGAATATCCCGCCCTGGAGAATCCCGGTGCCGAGGCCGCTCAATTGGTCGTAGACAGC
TCTAGCACCGCTTAAACGCACGTACGCGCTGTCCCCCGCGTTTTAACCGCCAAGGGGATTACTC
CCTAGTCTCCAGGCACGTGTCAGATATATACATCCTGTGCATGTAACTAGAGAATATCCCGCCC
TGGAGAATCCCGGTGCCGAGGCCGCTCAATTGGTCGTAGACAGCTCTAGCACCGCTTAAACGCA
CGTACGCGCTGTCCCCCGCGTTTTAACCGCCAAGGGGATTACTCCCTAGTCTCCAGGCACGTGT
CAGATATATACATCCTGTGCATGTAACTAGAGAATATCCCGCCCTGGAGAATCCCGGTGCCGAG
GCCGCTCAATTGGTCGTAGACAGCTCTAGCACCGCTTAAACGCACGTACGCGCTGTCCCCCGCG
TTTTAACCGCCAAGGGGATTACTCCCTAGTCTCCAGGCACGTGTCAGATATATACATCCTGTGC
ATGTAACTAGAGAATATCCCGCCCTGGAGAATCCCGGTGCCGAGGCCGCTCAATTGGTCGTAGA
CAGCTCTAGCACCGCTTAAACGCACGTACGCGCTGTCCCCCGCGTTTTAACCGCCAAGGGGATT
ACTCCCTAGTCTCCAGGCACGTGTCAGATATATACATCCTGTGCATGTAACTAGAGAATATCCC
GCCCTGGAGAATCCCGGTGCCGAGGCCGCTCAATTGGTCGTAGACAGCTCTAGCACCGCTTAAA
CGCACGTACGCGCTGTCCCCCGCGTTTTAACCGCCAAGGGGATTACTCCCTAGTCTCCAGGCAC
GTGTCAGATATATACATCCTGTGCATGTAACTAGAGAATATCCCGCCCTGGAGAATCCCGGTGC
CGAGGCCGCTCAATTGGTCGTAGACAGCTCTAGCACCGCTTAAACGCACGTACGCGCTGTCCCC
CGCGTTTTAACCGCCAAGGGGATTACTCCCTAGTCTCCAGGCACGTGTCAGATATATACATCCT
GTGCATGTAACTAGAGAATATCCCGCCCTGGAGAATCCCGGTGCCGAGGCCGCTCAATTGGTCG
TAGACAGCTCTAGCACCGCTTAAACGCACGTACGCGCTGTCCCCCGCGTTTTAACCGCCAAGGG
GATTACTCCCTAGTCTCCAGGCACGTGTCAGATATATACATCCTGTGCATGTAACTAGAGAATA
TCCCGCCCTGGAGAATCCCGGTGCCGAGGCCGCTCAATTGGTCGTAGACAGCTCTAGCACCGCT
TAAACGCACGTACGCGCTGTCCCCCGCGTTTTAACCGCCAAGGGGATTACTCCCTAGTCTCCAG
GCACGTGTCAGATATATACATCCTGTGCATGTAACTAGAGAATATCCCGCCCTGGAGAATCCCG
GTGCCGAGGCCGCTCAATTGGTCGTAGACAGCTCTAGCACCGCTTAAACGCACGTACGCGCTGT
CCCCCGCGTTTTAACCGCCAAGGGGATTACTCCCTAGTCTCCAGGCACGTGTCAGATATATACA
TCCTGTGCATGTAACTAGAGAATATCCCGCCCTGGAGAATCCCGGTGCCGAGGCCGCTCAATTG
GTCGTAGACAGCTCTAGCACCGCTTAAACGCACGTACGCGCTGTCCCCCGCGTTTTAACCGCCA
AGGGGATTACTCCCTAGTCTCCAGGCACGTGTCAGATATATACATCCTGTGCATGTAACTAGTT
ATCGCATGCAAGCTTGGCGTAATCATGGTCATAGCTGTTTCCTGTGTGAAATTGTTATCCGCTC
ACAATTCCACACAACATACGAGCCGGAAGCATAAAGTGTAAAGCCTGGGGTGCCTAATGAGTGA
GCTAACTCACATTAATTGCGTTGCGCTCACTGCCCGCTTTCCAGTCGGGAAACCTGTCGTGCCA
GCTGCATTAATGAATCGGCCAACGCGCGGGGAGAGGCGGTTTGCGTATTGGGCGCTCTTCCGCT
TCCTCGCTCACTGACTCGCTGCGCTCGGTCGTTCGGCTGCGGCGAGCGGTATCAGCTCACTCAA
AGGCGGTAATACGGTTATCCACAGAATCAGGGGATAACGCAGGAAAGAACATGTGAGCAAAAGG
CCAGCAAAAGGCCAGGAACCGTAAAAAGGCCGCGTTGCTGGCGTTTTTCCATAGGCTCCGCCCC
CCTGACGAGCATCACAAAAATCGACGCTCAAGTCAGAGGTGGCGAAACCCGACAGGACTATAAA
GATACCAGGCGTTTCCCCCTGGAAGCTCCCTCGTGCGCTCTCCTGTTCCGACCCTGCCGCTTAC
CGGATACCTGTCCGCCTTTCTCCCTTCGGGAAGCGTGGCGCTTTCTCATAGCTCACGCTGTAGG
TATCTCAGTTCGGTGTAGGTCGTTCGCTCCAAGCTGGGCTGTGTGCACGAACCCCCCGTTCAGC
CCGACCGCTGCGCCTTATCCGGTAACTATCGTCTTGAGTCCAACCCGGTAAGACACGACTTATC

GCCACTGGCAGCAGCCACTGGTAACAGGATTAGCAGAGCGAGGTATGTAGGCGGTGCTACAGAG
TTCTTGAAGTGGTGGCCTAACTACGGCTACACTAGAAGAACAGTATTTGGTATCTGCGCTCTGC
TGAAGCCAGTTACCTTCGGAAAAAGAGTTGGTAGCTCTTGATCCGGCAAACAAACCACCGCTGG
TAGCGGTGGTTTTTTTGTTTGCAAGCAGCAGATTACGCGCAGAAAAAAAGGATCTCAAGAAGAT
CCTTTGATCTTTTCTACGGGGTCTGACGCTCAGTGGAACGAAAACTCACGTTAAGGGATTTTGG
TCATGAGATTATCAAAAAGGATCTTCACCTAGATCCTTTTAAATTAAAAATGAAGTTTTAAATC
AATCTAAAGTATATATGAGTAAACTTGGTCTGACAGTTACCAATGCTTAATCAGTGAGGCACCT
ATCTCAGCGATCTGTCTATTTCGTTCATCCATAGTTGCCTGACTCCCCGTCGTGTAGATAACTA
CGATACGGGAGGGCTTACCATCTGGCCCCAGTGCTGCAATGATACCGCGAGACCCACGCTCACC
GGCTCCAGATTTATCAGCAATAAACCAGCCAGCCGGAAGGGCCGAGCGCAGAAGTGGTCCTGCA
ACTTTATCCGCCTCCATCCAGTCTATTAATTGTTGCCGGGAAGCTAGAGTAAGTAGTTCGCCAG
TTAATAGTTTGCGCAACGTTGTTGCCATTGCTACAGGCATCGTGGTGTCACGCTCGTCGTTTGG
TATGGCTTCATTCAGCTCCGGTTCCCAACGATCAAGGCGAGTTACATGATCCCCCATGTTGTGC
AAAAAAGCGGTTAGCTCCTTCGGTCCTCCGATCGTTGTCAGAAGTAAGTTGGCCGCAGTGTTAT
CACTCATGGTTATGGCAGCACTGCATAATTCTCTTACTGTCATGCCATCCGTAAGATGCTTTTC
TGTGACTGGTGAGTACTCAACCAAGTCATTCTGAGAATAGTGTATGCGGCGACCGAGTTGCTCT
TGCCCGGCGTCAATACGGGATAATACCGCGCCACATAGCAGAACTTTAAAAGTGCTCATCATTG
GAAAACGTTCTTCGGGGCGAAAACTCTCAAGGATCTTACCGCTGTTGAGATCCAGTTCGATGTA
ACCCACTCGTGCACCCAACTGATCTTCAGCATCTTTTACTTTCACCAGCGTTTCTGGGTGAGCA
AAAACAGGAAGGCAAAATGCCGCAAAAAAGGGAATAAGGGCGACACGGAAATGTTGAATACTCA
TACTCTTCCTTTTTCAATATTATTGAAGCATTTATCAGGGTTATTGTCTCATGAGCGGATACAT
ATTTGAATGTATTTAGAAAAATAAACAAATAGGGGTTCCGCGCACATTTCCCCGAAAAGTGCCA
CCTGACGTCTAAGAAACCATTATTATCATGACATTAACCTATAAAAATAGGCGTATCACGAGGC
CCTTTCGTC 3'

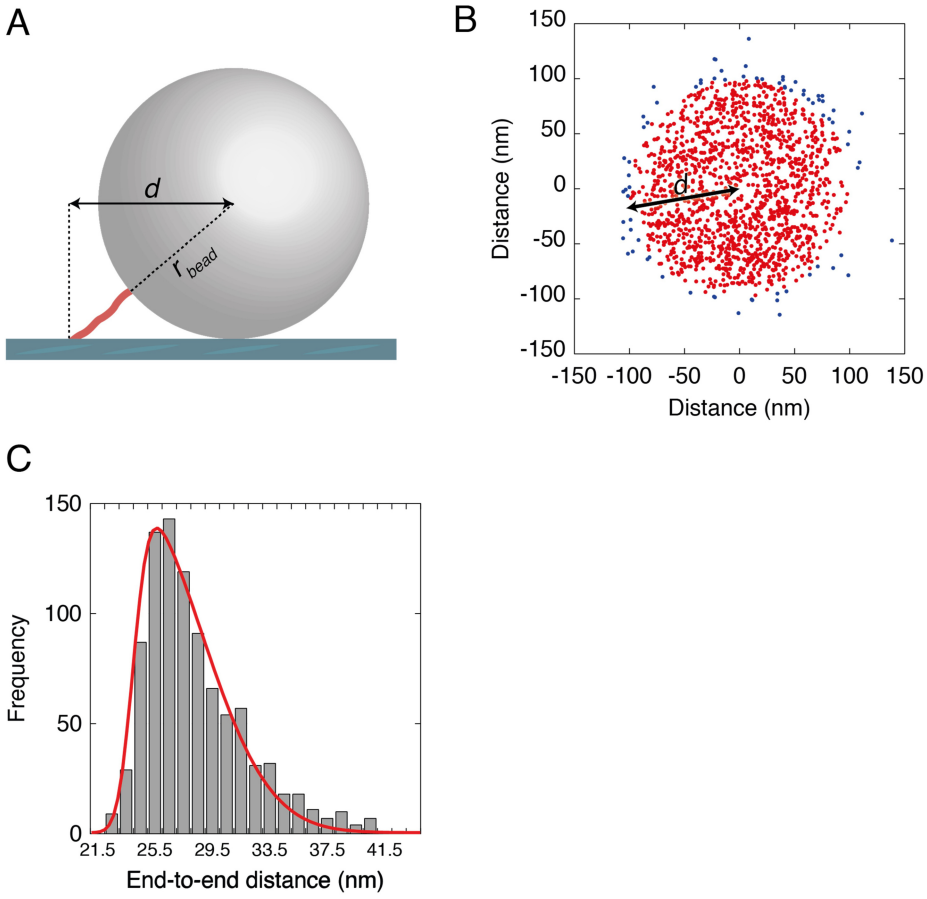

Figure 6.S1

End-to-end distance of the HMfB-DNA complex using TPM. A) Schematic drawing of the parameters used in the calculation of the end-to-end distance. d is the horizontal distance between the center of the bead and the place where the DNA is attached to the flow cell; r_{bead} is the radius of the bead. B) Positions of the TPM bead over 60 seconds at 50 nM HMfB (red dots). The 2.5% positions at the extremities of the plot (blue dots) represent the end-to-end distance of the HMfB-DNA complex. C) Skewed Gaussian fit (red line) of the end-to-end distance of the 2.5% most distant positions with respect to the center of 25 beads.

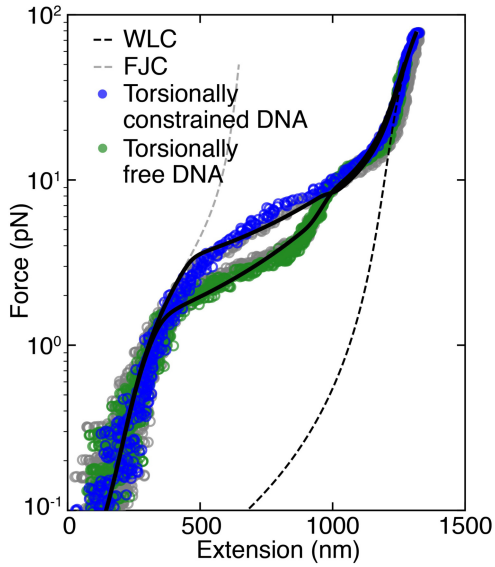

Figure 6.S2

Force spectroscopy on a torsionally constrained and a torsionally free HMfB-DNA complex. At low force ($F < 2$ pN) both complexes were identical in length, and the curve overlapped with the freely-jointed chain model (FJC). At high force ($F > 20$ pN) the curves overlapped with the worm-like chain model (WLC) of bare DNA. In between, the hypernucleosome unstacked and subsequently unwrapped. Due to the chiral structure of the hypernucleosome, unstacking induces torque, which stabilized the structure. The torsionally constrained hypernucleosome unstacked at $\sim$ 10 pN, compared to $\sim$ 1.5 pN for the torsionally unconstrained hypernucleosome. The unwrapping transition appeared unaffected. Fitting the torsionally constrained hypernucleosome yielded a higher stacking energy (4.2 ± 0.1 k_BT vs 1.6 ± 0.1 k_BT per dimer), reflecting an increased energy cost for unstacking the hypernucleosome. The wrapping energy was largely unaffected (9.9 ± 0.1 k_BT vs 10.0 ± 0.1 k_BT per dimer). The fit, however deviated somewhat from the data in the transition region. Both molecules appeared to contain 103 HMfB dimers, from which 95 were stacked in a hypernucleosome. The force-extension curves of both molecules converged to a WLC with a contour length of 3646 base pairs at forces over 30 pN.

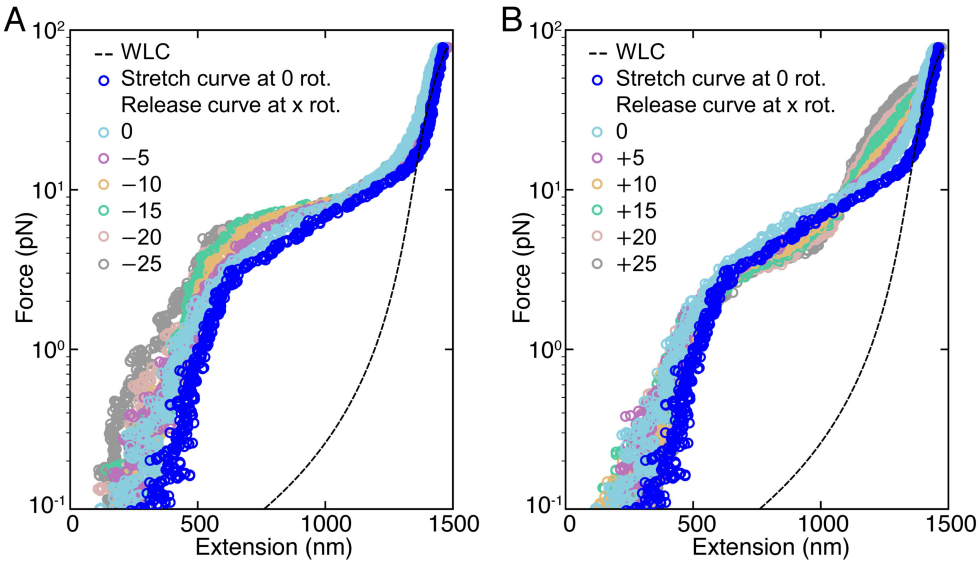

Figure 6.S3

Release curves of torsionally constrained HMfB-DNA complexes. A) Force spectroscopy on negatively twisted HMfB-DNA complexes. The release curves suggest that overtwisted DNA has a higher affinity to wrap DNA onto the HMfB dimers compared to relaxed DNA, shown by the reduced extension of the release curve. As a reference, the stretch curve for 0 twist was added in bright blue. Upon negative twist, the hysteresis reduced. B) Force spectroscopy experiments on positively twisted HMfB-DNA complexes. At forces between 10 and 40 pN the extension was reduced with increasing twist, which was also observed in the pulling curve.

Bibliography VI

[1] Tom A Williams et al. "An archaeal origin of eukaryotes supports only two primary domains of life". In: *Nature* 504.7479 (2013), p. 231.

[2] Katarzyna Zaremba-Niedzwiedzka et al. "Asgard archaea illuminate the origin of eukaryotic cellular complexity". In: *Nature* 541.7637 (2017), p. 353.

[3] Laura Eme et al. "Archaea and the origin of eukaryotes". In: *Nature Reviews Microbiology* 15.12 (2017), p. 711.

[4] Cymon J Cox et al. "The archaebacterial origin of eukaryotes". In: *Proceedings of the National Academy of Sciences* 105.51 (2008), pp. 20356–20361.

[5] Gregory D Bowman and Michael G Poirier. "Post-Translational Modi fi cations of Histones That In fl uence Nucleosome Dynamics". In: *Chemical Reviews* 115 (2015), pp. 2274–2295. ISSN: 0009-2665. DOI: 10.1021/cr500350x.

[6] Kathleen Sandman and John N Reeve. "Archaeal chromatin proteins: different structures but common function?" In: *Current opinion in microbiology* 8.6 (2005), pp. 656–661.

[7] Eveline Peeters et al. "The interplay between nucleoid organization and transcription in archaeal genomes". In: *Nature Reviews Microbiology* 13.6 (2015), p. 333.

[8] Martijn S Luijsterburg et al. "The major architects of chromatin: architectural proteins in bacteria, archaea and eukaryotes". In: *Critical reviews in biochemistry and molecular biology* 43.6 (2008), pp. 393–418.

[9] Erin A Becker et al. "Phylogenetically driven sequencing of extremely halophilic archaea reveals strategies for static and dynamic osmo-response". In: *PLoS genetics* 10.11 (2014), e1004784.

[10] Carol J Bult et al. "Complete genome sequence of the methanogenic archaeon, Methanococcus jannaschii". In: *Science* 273.5278 (1996), pp. 1058–1073.

[11] Trevor J Darcy, Kathleen Sandman, and John N Reeve. "Methanobacterium formicicum, a mesophilic methanogen, contains three HFo histones." In: *Journal of bacteriology* 177.3 (1995), pp. 858–860.

[12] R Tabassum, KM Sandman, and JN Reeve. "HMt, a histone-related protein from Methanobacterium thermoautotrophicum delta H." In: *Journal of bacteriology* 174.24 (1992), pp. 7890–7895.

[13] Bram Henneman and Remus T. Dame. "Archaeal histones: dynamic and versatile genome architects". In: *AIMS Microbiology* 1.1 (2015), pp. 72–81. ISSN: 2471-1888. DOI: 10.3934/microbiol.2015.1.72.

[14] Toshiaki Fukui et al. “Complete genome sequence of the hyperthermophilic archaeon Thermococcus kodakaraensis KOD1 and comparison with Pyrococcus genomes”. In: *Genome research* 15.3 (2005), pp. 352–363.

[15] Iain Anderson et al. “Complete genome sequence of Methanothermus fervidus type strain (V24S T)”. In: *Standards in genomic sciences* 3.3 (2010), p. 315.

[16] K Sandman et al. “HMf, a DNA-binding protein isolated from the hyperthermophilic archaeon Methanothermus fervidus, is most closely related to histones.” In: *Proceedings of the National Academy of Sciences* 87.15 (1990), pp. 5788–5791.

[17] Kathleen Sandman et al. “Growth-phase-dependent synthesis of histones in the archaeon Methanothermus fervidus”. In: *Proceedings of the National Academy of Sciences* 91.26 (1994), pp. 12624–12628.

[18] David R Musgrave, Kathleen M Sandman, and John N Reeve. “DNA binding by the archaeal histone HMf results in positive supercoiling”. In: *Proceedings of the National Academy of Sciences* 88.23 (1991), pp. 10397–10401.

[19] Rowan A Grayling, Kathleen Sandman, and John N Reeve. “DNA stability and DNA binding proteins”. In: *Advances in protein chemistry*. Vol. 48. Elsevier, 1996, pp. 437–467.

[20] Frédéric Marc et al. “Archaeal histone tetramerization determines DNA affinity and the direction of DNA supercoiling”. In: *Journal of Biological Chemistry* 277.34 (2002), pp. 30879–30886.

[21] MT Howard et al. “HMf, a histone-related protein from the hyperthermophilic archaeon Methanothermus fervidus, binds preferentially to DNA containing phased tracts of adenines.” In: *Journal of bacteriology* 174.23 (1992), pp. 7864–7867.

[22] Narasimharao Nalabothula et al. “Archaeal nucleosome positioning in vivo and in vitro is directed by primary sequence motifs”. In: *BMC genomics* 14.1 (2013), p. 391.

[23] Kathryn A Bailey et al. “Archaeal histone selection of nucleosome positioning sequences and the procaryotic origin of histone-dependent genome evolution”. In: *Journal of molecular biology* 303.1 (2000), pp. 25–34.

[24] Kathryn A Bailey et al. “Both DNA and histone fold sequences contribute to archaeal nucleosome stability”. In: *Journal of Biological Chemistry* 277.11 (2002), pp. 9293–9301.

[25] Francesca Mattiroli et al. “Structure of histone-based chromatin in Archaea”. In: *Science* 357.6351 (2017), pp. 609–612. ISSN: 0036-8075. DOI: 10.1126/science.aaj1849.

[26] Bram Henneman et al. “Structure and function of archaeal histones”. In: *PLoS genetics* 14.9 (2018), e1007582.

[27] Ron Ammar et al. “Chromatin is an ancient innovation conserved between Archaea and Eukarya”. In: *elife* 1 (2012), e00078.

[28] Hugo Maruyama et al. “An alternative beads-on-a-string chromatin architecture in Thermococcus kodakarensis”. In: *EMBO reports* 14.8 (2013), pp. 711–717.

[29] Artem K Efremov et al. “Transcriptional repressor TrmBL2 from Thermococcus kodakarensis forms filamentous nucleoprotein structures and competes with histones for DNA binding in a salt-and DNA supercoiling-dependent manner”. In: *Journal of Biological Chemistry* 290.25 (2015), pp. 15770–15784.

[30] David Musgrave, Patrick Forterre, and Alexei Slesarev. “Negative constrained DNA supercoiling in archaeal nucleosomes”. In: *Molecular microbiology* 35.2 (2000), pp. 341–349.

[31] Rosalie PC Driessen et al. “Effect of temperature on the intrinsic flexibility of DNA and its interaction with architectural proteins”. In: *Biochemistry* 53.41 (2014), pp. 6430–6438.

[32] Rosalie PC Driessen et al. “Diverse architectural properties of Sso10a proteins: Evidence for a role in chromatin compaction and organization”. In: *Scientific reports* 6 (2016), p. 29422.

[33] Rosalie PC Driessen et al. “Crenarchaeal chromatin proteins Cren7 and Sul7 compact DNA by inducing rigid bends”. In: *Nucleic acids research* 41.1 (2012), pp. 196–205.

[34] Ramon A van der Valk, Niels Laurens, and Remus T Dame. “Tethered particle motion analysis of the DNA binding properties of architectural proteins”. In: *The Bacterial Nucleoid*. Springer, 2017, pp. 127–143.

[35] Miroslav Tomschik et al. “The archaeal histone-fold protein HMf organizes DNA into bona fide chromatin fibers”. In: *Structure* 9.12 (2001), pp. 1201–1211.

[36] Yingang Feng, Hongwei Yao, and Jinfeng Wang. “Crystal structure of the crenarchaeal conserved chromatin protein Cren7 and double-stranded DNA complex”. In: *Protein Science* 19.6 (2010), pp. 1253–1257.

[37] Liqing Chen et al. “The hyperthermophile protein Sso10a is a dimer of winged helix DNA-binding domains linked by an antiparallel coiled coil rod”. In: *Journal of molecular biology* 341.1 (2004), pp. 73–91.

[38] Igor M. Kulić et al. “Equation of state of looped DNA”. In: *Physical Review E - Statistical, Nonlinear, and Soft Matter Physics* 75.1 (2007). ISSN: 15393755. DOI: 10.1103/PhysRevE.75.011913. arXiv: 0509003 [q-bio].

[39] J. van Noort et al. “Dual architectural roles of HU: Formation of flexible hinges and rigid filaments”. In: *Proceedings of the National Academy of Sciences* 101.18 (2004), pp. 6969–6974. ISSN: 0027-8424. DOI: 10.1073/pnas.0308230101.

[40] He Meng, Kurt Andresen, and John van Noort. “Quantitative analysis of single-molecule force spectroscopy on folded chromatin fibers”. In: *Nucleic Acids Research* 43.7 (Apr. 2015), pp. 3578–3590. ISSN: 13624962. DOI: 10.1093/nar/gkv215.

[41] GCP Van Zundert et al. “The HADDOCK2. 2 web server: user-friendly integrative modeling of biomolecular complexes”. In: *Journal of molecular biology* 428.4 (2016), pp. 720–725.

[42] Klaas Decanniere et al. “Crystal structures of recombinant histones HMfA and HMfB from the hyperthermophilic archaeon Methanothermus fervidus”. In: *Journal of molecular biology* 303.1 (2000), pp. 35–47.

[43] Divya J Soares, Kathleen Sandman, and John N Reeve. "Mutational analysis of archaeal histone-DNA interactions". In: *Journal of molecular biology* 297.1 (2000), pp. 39–47.

[44] Kathleen Sandman and John N Reeve. "Chromosome packaging by archaeal histones". In: *Adv. Appl. Microbiol* 50 (2001), pp. 75–99.

[45] Jan Lipfert, Sven Klijnhout, and Nynke H Dekker. "Torsional sensing of small-molecule binding using magnetic tweezers". In: *Nucleic acids research* 38.20 (2010), pp. 7122–7132.

[46] Artur Kaczmarczyk et al. "Single-molecule force spectroscopy on histone H4 tail-cross-linked chromatin reveals fiber folding". In: *Journal of Biological Chemistry* 292.42 (2017), pp. 17506–17513.

[47] Travis J Sanders et al. "TFS and Spt4/5 accelerate transcription through archaeal histone-based chromatin". In: *Molecular microbiology* 111.3 (2019), pp. 784–797.

[48] Hiromi Nishida and Taku Oshima. "Archaeal histone distribution is associated with archaeal genome base composition". In: *The Journal of general and applied microbiology* 63.1 (2017), pp. 28–35.

[49] W Brent R Pollock et al. "Bacterial expression of a mitochondrial cytochrome c. Trimethylation of Lys72 in yeast iso-1-cytochrome c and the alkaline conformational transition". In: *Biochemistry* 37.17 (1998), pp. 6124–6131.

[50] P T T Lowary and J Widom. "New DNA sequence rules for high affinity binding to histone octamer and sequence-directed nucleosome positioning." In: *Journal of molecular biology* 276.1 (1998), pp. 19–42. ISSN: 0022-2836. DOI: 10.1006/jmbi.1997.1494. eprint: NIHMS150003.

[51] Thomas B Brouwer et al. "Unraveling DNA Organization with Single-Molecule Force Spectroscopy Using Magnetic Tweezers". In: *Bacterial Chromatin*. Springer, 2018, pp. 317–349.

[52] Bram Henneman et al. "Quantitation of DNA-binding affinity using Tethered Particle Motion". In: *Bacterial Chromatin*. Springer, 2018, pp. 257–275.

[53] TR Strick et al. "Physical approaches to the study of DNA". In: *Journal of statistical physics* 93.3-4 (1998), pp. 647–672.

[54] Terence Strick et al. "Twisting and stretching single DNA molecules". In: *Progress in biophysics and molecular biology* 74.1-2 (2000), pp. 115–140.

[55] John F. Marko and Eric D. Siggia. "Stretching DNA". In: *Macromolecules* 28.26 (Dec. 1995), pp. 8759–8770. ISSN: 15205835. DOI: 10.1021/ma00130a008.

[56] Suzette L Pereira et al. "Archaeal nucleosomes". In: *Proceedings of the National Academy of Sciences* 94.23 (1997), pp. 12633–12637.

[57] IM Kulić and Helmut Schiessel. "DNA spools under tension". In: *Physical Review Letters* 92.22 (2004), p. 228101.

[58] Carlos Bustamante, Zev Bryant, and Steven B. Smith. "Ten years of tension: single-molecule DNA mechanics". In: *Nature* 421.6921 (2003), pp. 423–427. ISSN: 0028-0836. DOI: 10.1038/nature01405.